Porous tablets of crystalline calcium carbonate via sintering of amorphous nanoparticles

Denis Gebauer, Xingmin Liu, Baroz Aziz, Niklas Hedin, and Zhe Zhao**

Supporting Information

Methods

***Single-Crystal Analysis*:** 2D X-ray diffraction patterns were collected on an Oxford Diffraction Xcalibur3 diffractometer with a Sapphire-3 CCD detector (Gaussian absorption correction). Fractured pieces (ca. 0.5 mm in diameter) from the surface and from the bulk of the sample processed at 300°C were exposed to the X-ray beam for 5 minutes.

Thermogravimetric Analysis (TGA): A Perkin Elmer Thermogravimetric Analyzer TGA7 was used to study the weight loss as a function of temperature. Powder of ACC (~10mg) was analyzed from 40°C to 800°C at a heating rate of 2°C/min. Crystalline calcium carbonate (~40mg) was analyzed from 40°C to 1000°C at a heating rate of 10°C/min. Samples were contained in platinum cups during TGA and analysed in a flow of dry air.

Figures

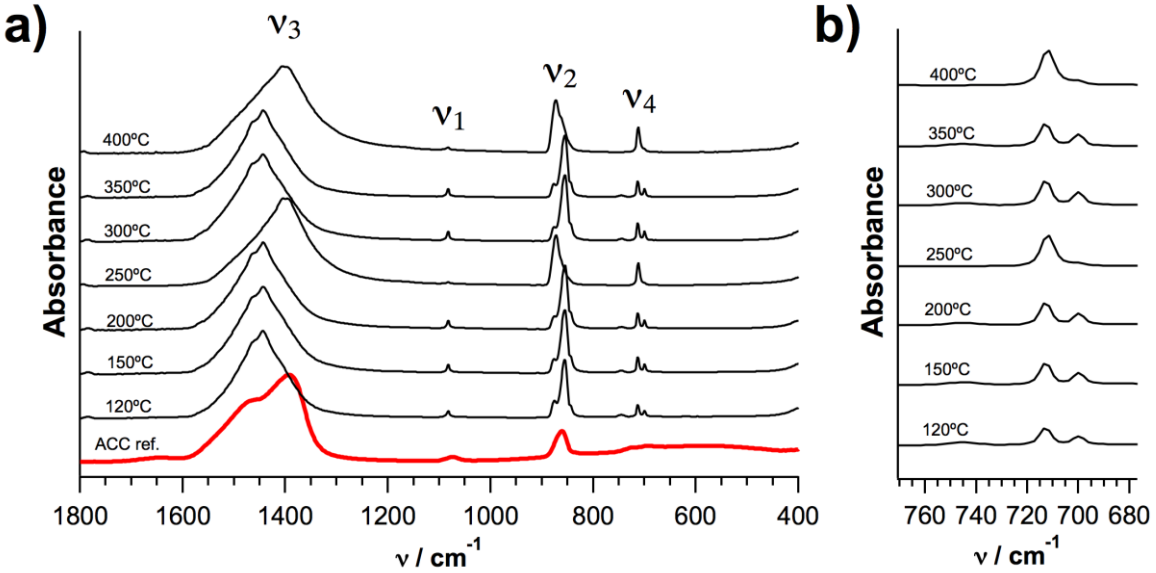

Figure S1. Fourier transform infrared spectra of the precursor powder (red bottom trace) and of powders obtained from the monoliths (a); traces are labeled with the sintering temperature. The spectra show features for vaterite, calcite, and aragonite (b): characteristic ν_4 modes are 744 cm^{-1} for vaterite (minor content), 712 cm^{-1} for calcite, and 700 cm^{-1} for aragonite (doublet superimposed with calcite). Samples from the surface (250°C) show enhanced spectral characteristics of calcite, as also evident from X-ray diffraction studies on intact tablets (see Figure S7). The relatively narrow bands corresponding to the ν_4 modes indicate the absence of significant amounts of amorphous calcium carbonate (ACC).

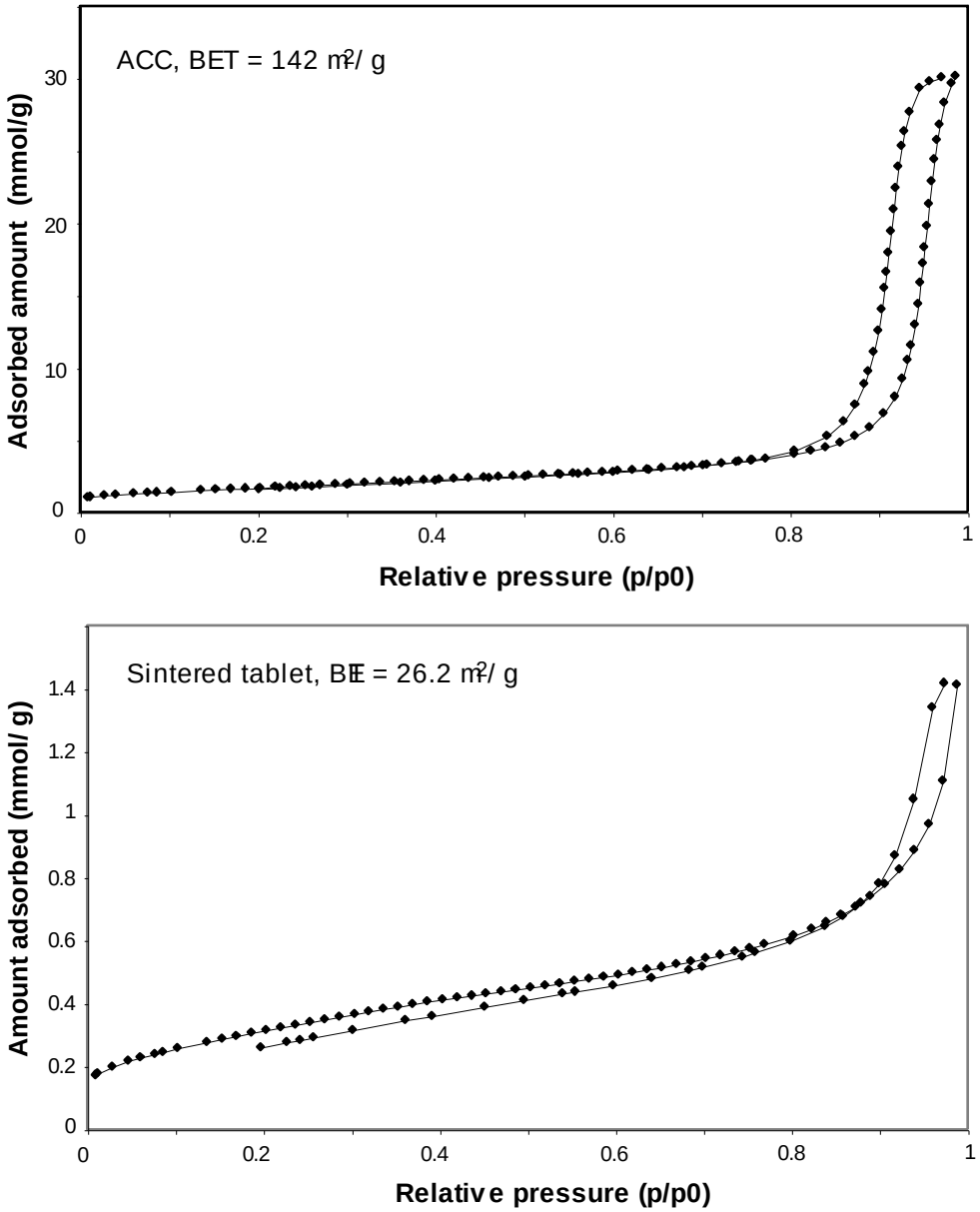

Figure S2. N_2 Brunauer-Emmett-Teller (BET) adsorption/ desorption isotherms (top) typical isotherms for amorphous precursor nanoparticles, (bottom) isotherms for a tablet sintered at 200 °C with a heating rate of 50 °C/ min.

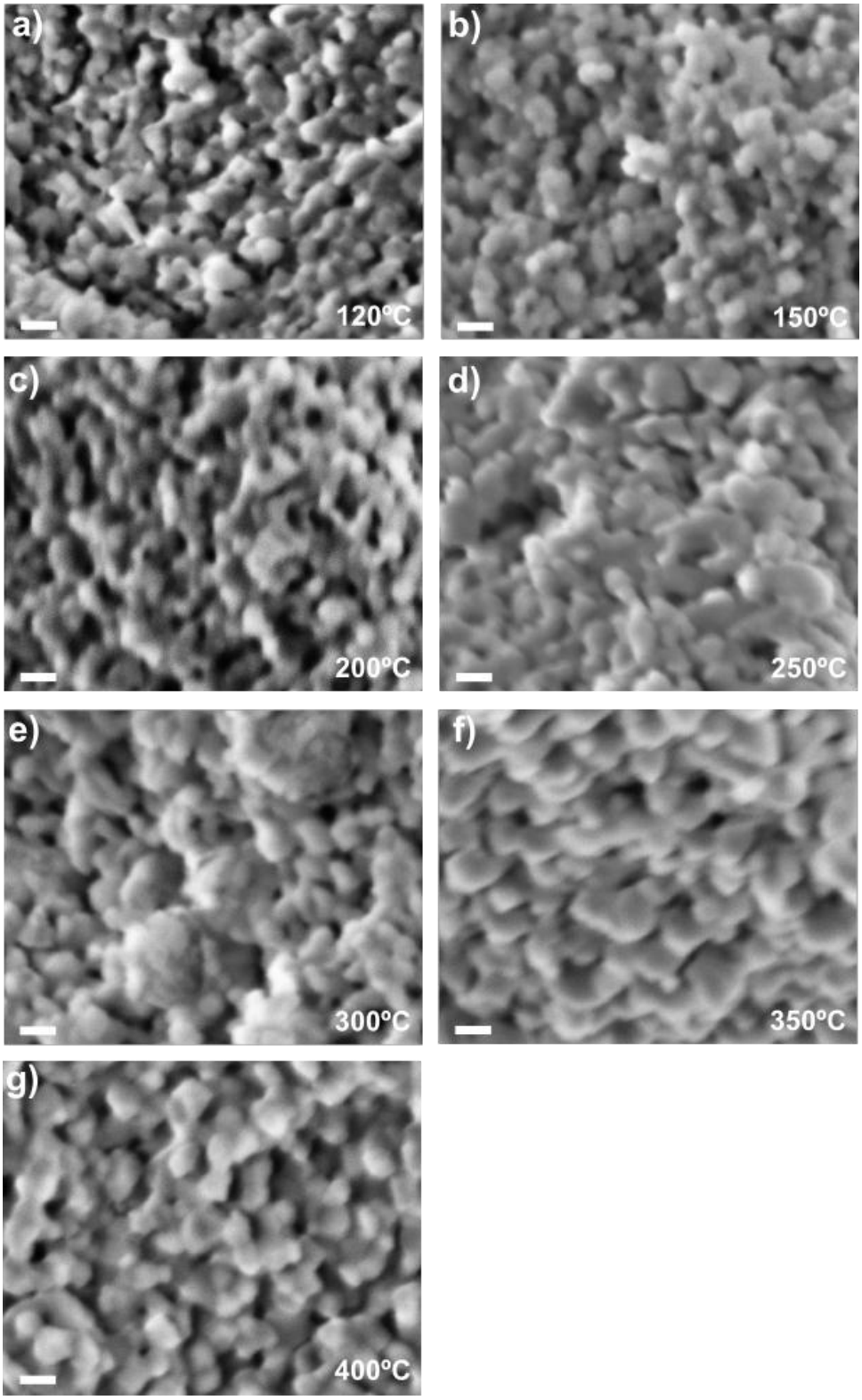

Figure S3. Scanning electron micrographs of fracture edges of porous monoliths of calcium carbonate at ×100,000 magnification. Sintering temperatures are indicated. Scale bars are 100 nm.

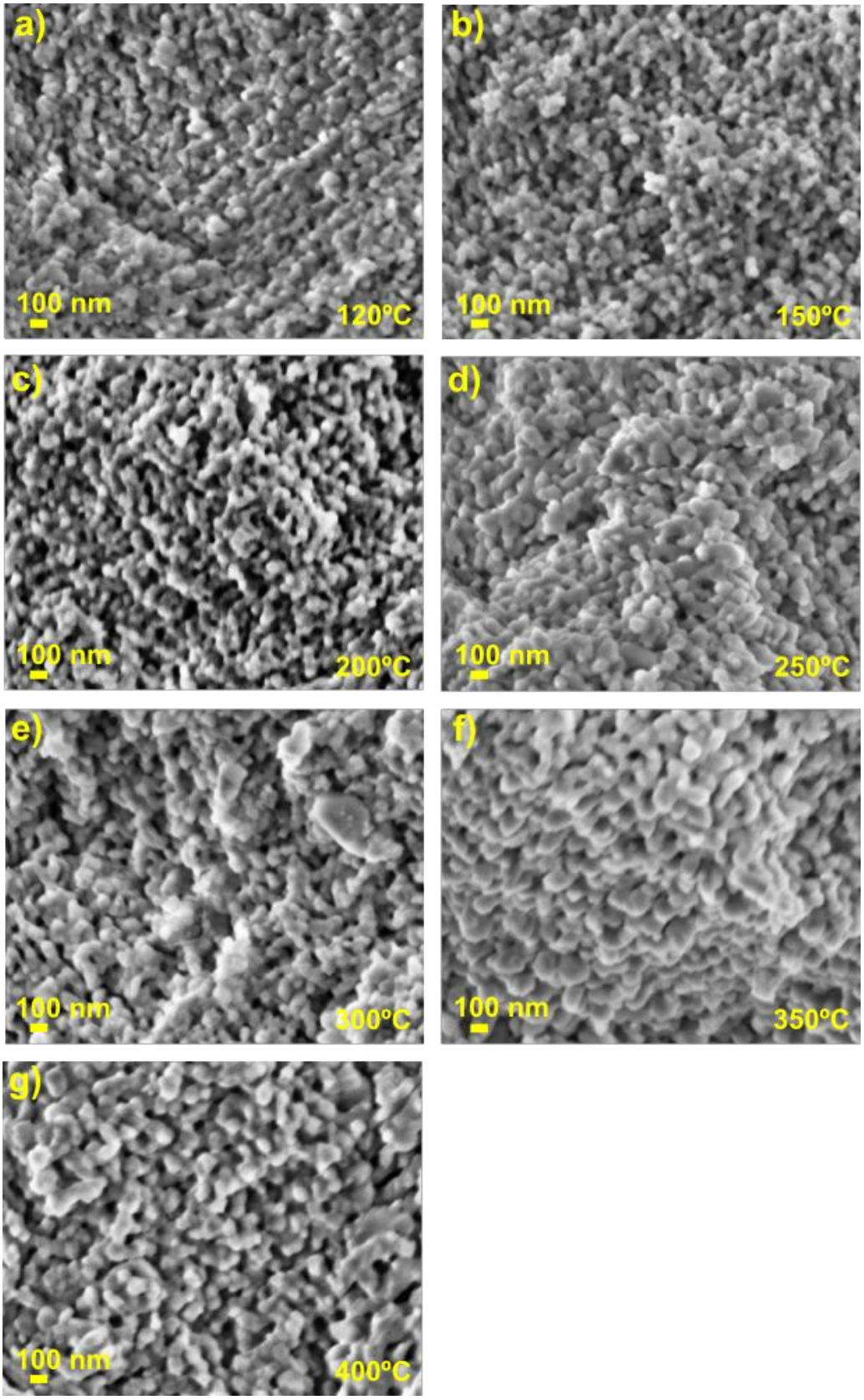

Figure S4. Scanning electron micrographs of fracture edges of porous monoliths of calcium carbonate at ×50,000 magnification. Sintering temperatures are indicated.

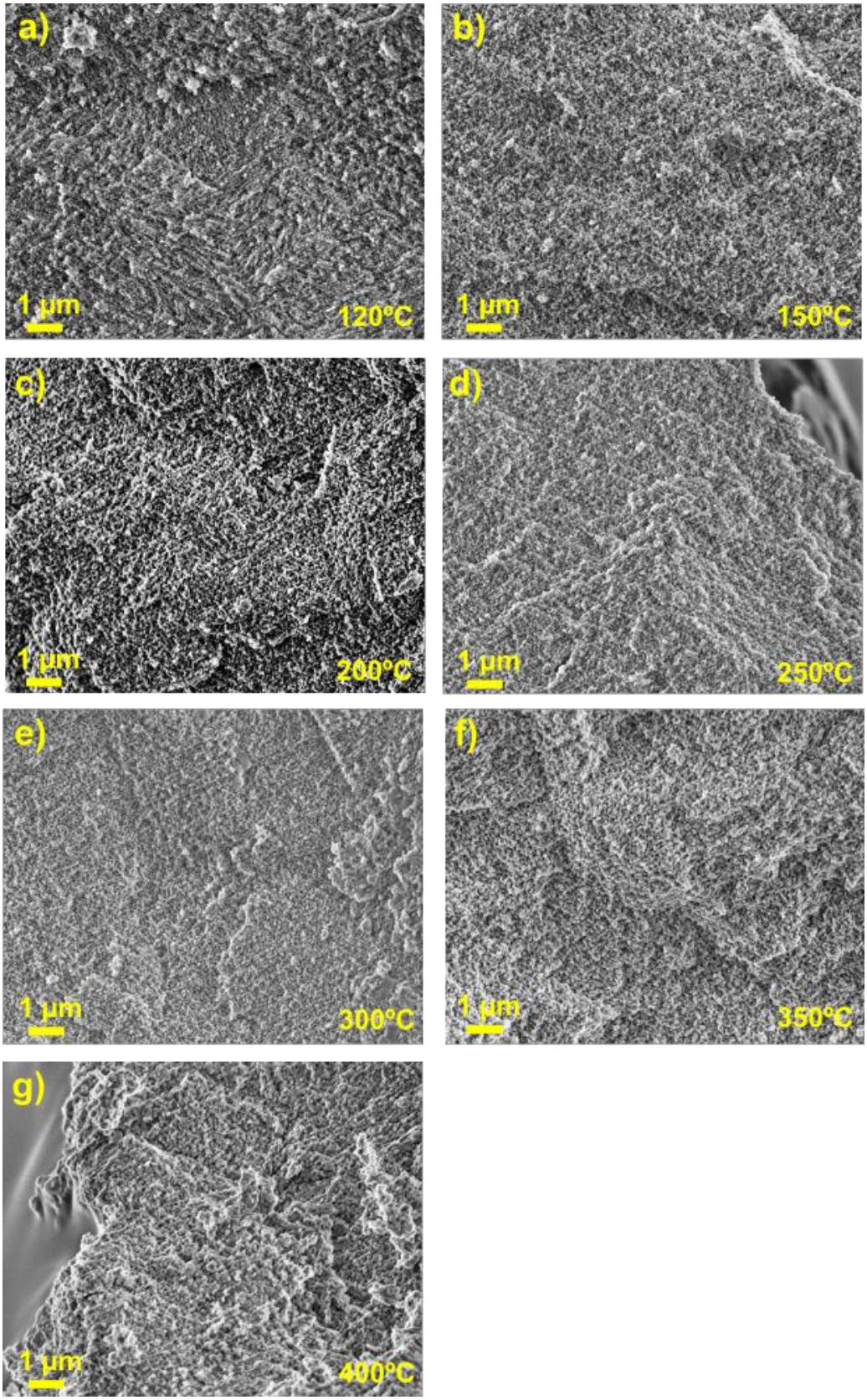

Figure S5. Scanning electron micrographs of fracture edges of porous monoliths of calcium carbonate at ×10,000 magnification. Sintering temperatures are indicated.

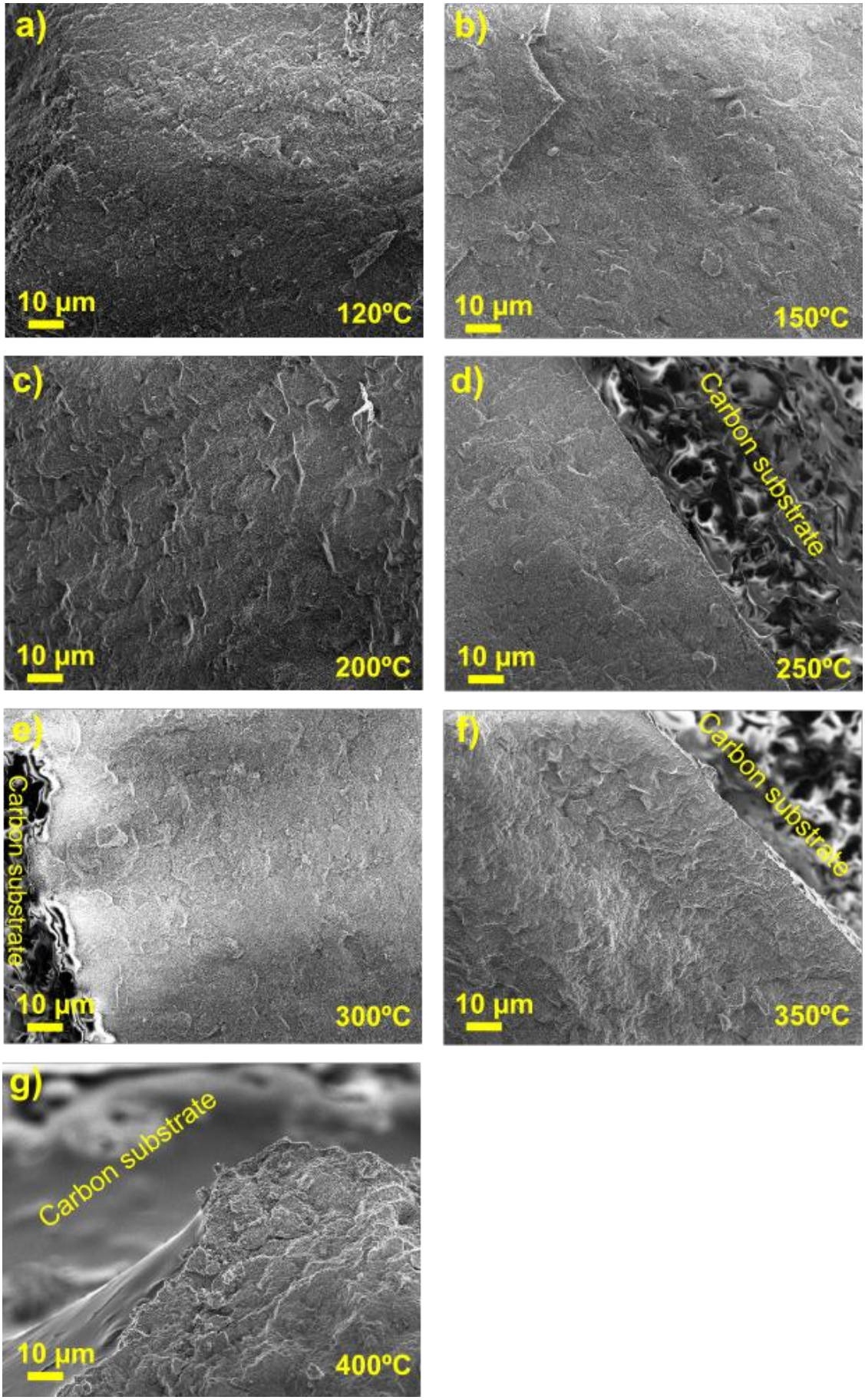

Figure S6. Scanning electron micrographs of fracture edges of porous monoliths of calcium carbonate at ×1,000 magnification. Sintering temperatures are indicated.

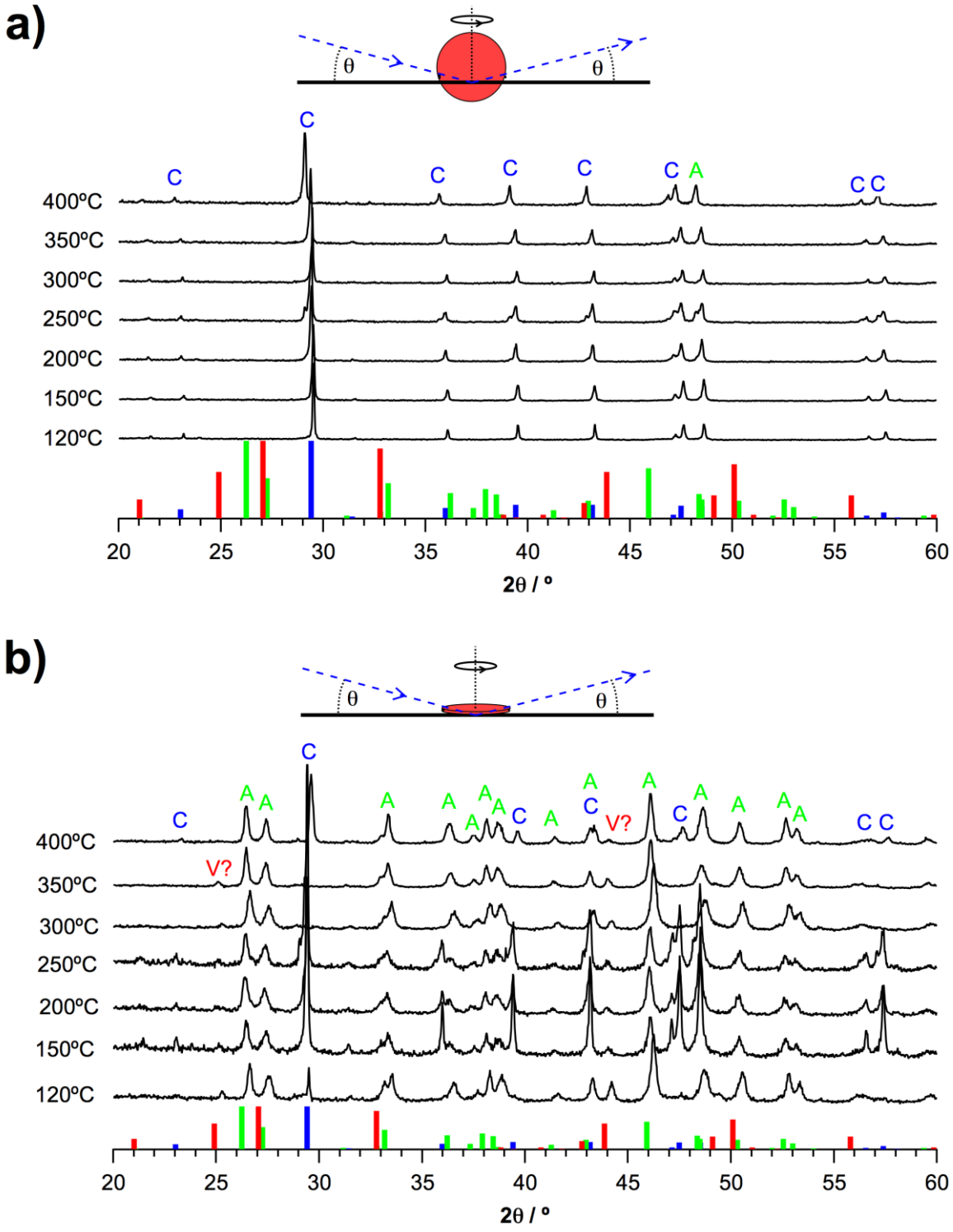

Figure S7. X-ray diffractograms of whole tablets, oriented as indicated in the cartoons, rotating vertically (a) and horizontally (b). The diffractograms are labeled with the respective processing temperatures, and were normalized to the most intense calcite reflection at ~29°. The database (ICDD) diffraction patterns of calcite (blue), vaterite (red), and aragonite (green) are shown at the bottom. Reflections are furthermore marked with C (calcite), V (vaterite), or A (aragonite). In both orientations, distinct amounts of calcite are detected (calcite is only detectable in fine-ground tablets in the case of the specimen processed at 400°C; Figure S10). Because the X-rays only penetrate the samples to shallow depths, we infer that calcite is solely formed near the surface, especially at the outer rim of the tablets.

Figure S8. A two-dimensional diffractogram obtained from a fractured piece from the bulk of a tablet sintered at 300°C. The observed ring pattern is representative of aragonite, and the individual crystallites show no obvious mutual alignment or orientation. An identical diffractogram was obtained from a fractured piece from the surface of the tablet (data not shown). Note that the diffractogram of the tiny specimen from the surface does not resemble the statistical significance of the diffractograms obtained from whole tablets shown in Figure S8. A distinct amorphous content would result in a halo around the beam stop, which is not observed. We infer that the content of amorphous calcium carbonate, if present, is negligibly small.

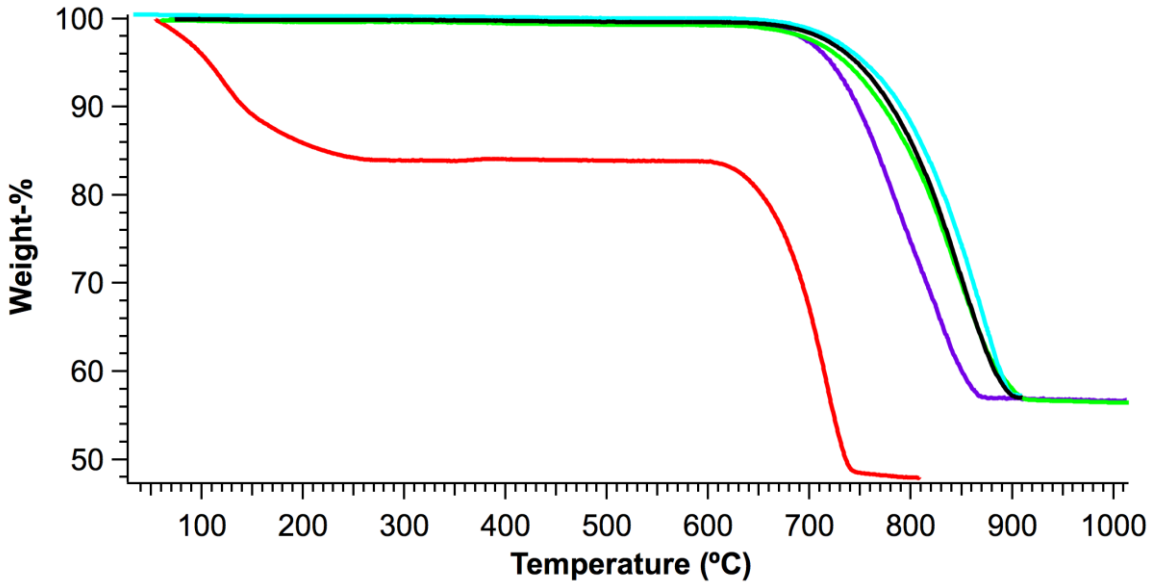

Figure S9. Thermogravimetric analysis (TGA) of the precursor powder of amorphous calcium carbonate (ACC, red trace) and of the monoliths processed at 120 ºC (mauve trace), 250 ºC (black trace), 300 ºC (green trace) and 400 ºC (cyan trace). The ACC may be considered as stoichiometric $CaCO_3 \cdot H_2O$, whereas the processed monoliths consist of pure $CaCO_3$. The theoretical weight loss for $CaCO_3 \cdot H_2O$ during heating in dry air may be expressed as follows: $CaCO_3 \cdot H_2O$ (118 u <=> 100%) → $CaCO_3 + H_2O\uparrow$ (100 u + 18 u↑ <=> 85% + 15%↑) → $CaO + CO_2\uparrow$ (56 u + 44 u↑ <=> 48% + 37%↑). In the case of decomposition and pure $CaCO_3$, the expected final weight is 56%. Structural water is released at temperatures between ~60°C and 200°C, and decomposition to calcium oxide and carbon dioxide starts at ~700°C for the powder of nanoparticles and at ~750°C for the mesoporous monoliths. Note that calibration of the TGA equipment used in this study does not provide high temperature-accuracy at elevated temperatures (at 700°C: $\Delta T \approx 50$°C).